

Short Communication

Disruption of gingipain oligomerization into non-covalent cell-surface attached complexes

Maryta Sztukowska^{1,2,a}, Florian Veillard^{1,a}, Barbara Potempa¹, Matthew Bogyo³, Jan J. Enghild⁴, Ida B. Thogersen⁴, Ky-Anh Nguyen^{5,6} and Jan Potempa^{1,7,*}

¹Oral Health and Systemic Diseases Research Group, University of Louisville School of Dentistry, Louisville, KY 40202, USA

²University of Information Technology and Management, 35-225 Rzeszow, Poland

³Departments of Pathology, and Microbiology and Immunology, Stanford University School of Medicine, Stanford, CA 94305, USA

⁴Center for Insoluble Protein Structures (inSPIN) and Interdisciplinary Nanoscience Center (iNANO) at the Department of Molecular Biology and Genetics, Aarhus University, DK-8000 Aarhus, Denmark

⁵Institute of Dental Research, Westmead Centre for Oral Health and Westmead Millenium Institute, Sydney 2145, NSW, Australia

⁶Faculty of Dentistry, University of Sydney, Sydney 2006, NSW, Australia

⁷Department of Microbiology, Faculty of Biochemistry, Biophysics and Biotechnology, Jagiellonian University, 30-387 Krakow, Poland

* Corresponding author
e-mail: jspot01@louisville.edu

Abstract

RgpA and Kgp gingipains are non-covalent complexes of endoprotease catalytic and hemagglutinin-adhesin domains on the surface of *Porphyromonas gingivalis*. A motif conserved in each domain has been suggested to function as an oligomerization motif. We tested this hypothesis by mutating motif residues to hexahistidine or insertion of hexahistidine tag to disrupt the motif within the Kgp catalytic domain. All modifications led to the secretion of entire Kgp activity into the growth media, predominantly in a form without functional His-tag. This confirmed the role of the conserved motif in correct posttranslational proteolytic processing and assembly of the multidomain complexes.

Keywords: cysteine protease; limited proteolysis; periodontitis; *Porphyromonas gingivalis*; posttranslational processing.

Arguably, periodontitis is the most prevalent infection-driven chronic inflammatory disorder of mankind and *Porphyromonas gingivalis* is considered the pivotal aetiologic organism responsible for the development and progression of the disease (Albandar and Rams, 2002; Cobb et al., 2009). This anaerobic, asaccharolytic Gram-negative bacterium is well armed with virulence factors and the gingipain cysteine protease family plays a key role in *P. gingivalis* pathogenesis (Guo et al., 2010). Except for one laboratory strain of *P. gingivalis* (HG66), which secretes soluble gingipains, in all other strains, the gingipains are associated with the bacterial outer membrane (Potempa et al., 1995). While Arg-specific gingipain B (RgpB) is a single chain protease (Mikolajczyk-Pawlinska et al., 1998), membrane-associated Lys-specific gingipain (Kgp) and Arg-specific gingipain A (RgpA) are assembled into very large (>300 kDa), multifunctional (Pathirana et al., 2008; Tam et al., 2008, 2009; O'Brien-Simpson et al., 2009), non-covalent complexes composed of two individual unique protease domains (RgpA_{cat} and Kgp_{cat}) and several hemagglutinin-adhesin domains (RgpA_{HA1}, Kgp_{HA1}, RgpA_{HA2}, Kgp_{HA2}, RgpA_{HA3}, and Kgp_{HA3}) (Bhogal et al., 1997) (Figure 1). All domains are generated by limited proteolysis of a single, nascent polypeptide chain encoded by *rgpA* or *kgp* genes, with the hemagglutinin-adhesin (HA) domains being located in the C-terminal extension of the translation products of the two genes (Pike et al., 1994; Pavloff et al., 1995, 1997). In addition, some adhesin domains in the complexes are derived from HagA (Pathirana et al., 2006), a large protein encompassing up to 4 HA-domain repeats (Kozarov et al., 1998). With the exception of Lys-Pro peptide bond being cleaved downstream of the hemoglobin-binding domain (HA2), the initial proteolytic processing of other domains occurs at Arg-Xaa peptide bonds (Figure 1). The initial cleavage is followed by progressive truncation of the C-terminus at Lys-Xaa sites by Kgp and removal of the resulting C-terminal Lys by a surface located carboxypeptidase (Figure 1) (Veith et al., 2002, 2004). Individual domains generated in this sequence of proteolytic events remain tightly associated via non-covalent, protein-protein interactions.

A conserved sequence (PVxNLT) present on the catalytic, HA1 and HA3 domains referred to as the adhesin-binding motif (ABM); was suggested to be responsible for oligomerization and assembly of multidomain complexes (Slakeski et al., 1998). To test this hypothesis, we have disrupted this motif in Kgp_{cat} by insertion of hexahistidine residues or by mutation of six consecutive residues of ABM into histidine residues (Figure 1). The accuracy of these genetic manipulations was confirmed by DNA resequencing of the entire *kgp* gene and secretion of gingipains by different mutants

^aThese authors contributed equally to this study.

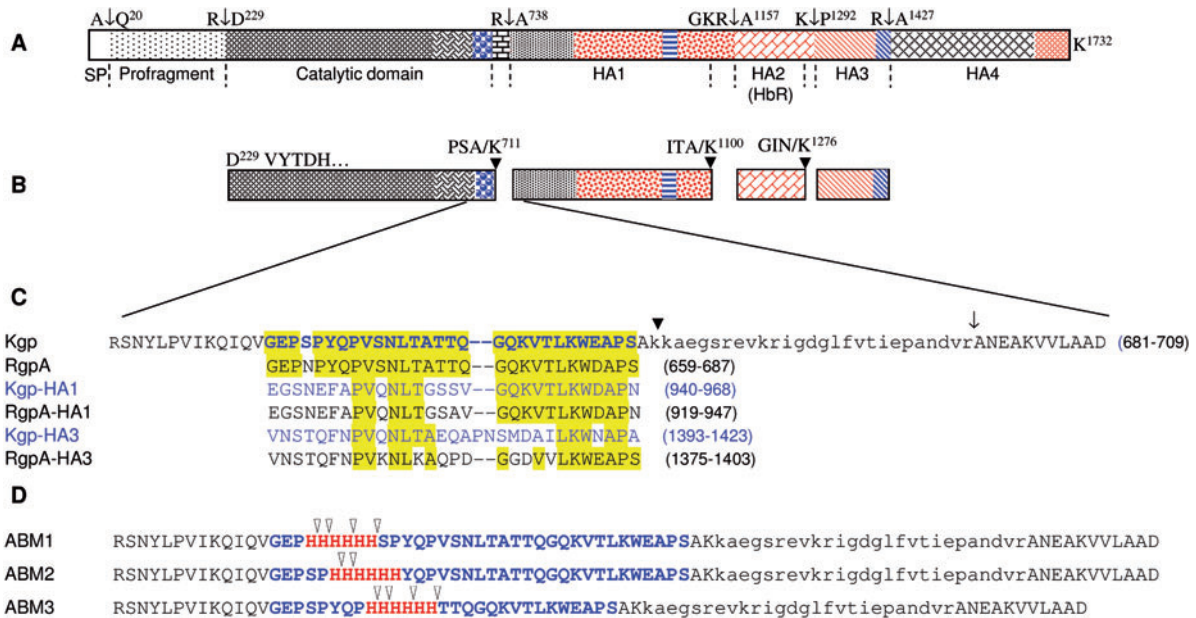


Figure 1 Schematic representation of preproKgp posttranslational proteolytic processing into catalytic and hemagglutinin/adhesin (HA) domains in *P. gingivalis* strain W83.

The nascent translation product of the *rgpA* gene has the same subdomain structure as preproKgp and the polyprotein is processed in the same way as proKgp (Pavloff et al., 1995, 1997). Parts of the polypeptide chain with sequence identity over 95% in Kgp and RgpA are highlighted red. Initial proteolysis releases individual domains from the polyprotein (A) is followed by progressive truncation of the C-terminus at indicated Lys-Xaa peptide bonds in the catalytic, HA1 and HA2 domains (B). Subsequently, C-terminal lysines are removed by a carboxypeptidase (Veith et al., 2002, 2004). The cleavage sites at the Kgp_{cat}-HA1 junction are enlarged in panel C. Lowercase sequence indicates the region absent in the non-covalent complex of Kgp_{cat} and HA domains. Blue shaded regions denote the adhesin binding motifs (ABM), which have been proposed to mediate protein-protein interaction between the various domains. Verification of the ABM role in oligomerization of gingipain domains was tested by disruption of the ABM motif located in the catalytic domain by insertion of hexahistidine tag or replacement of ABM residues with hexahistidine (D). In ABM1 and ABM2 mutants, hexahistidine tag was inserted after Pro683 and Pro685, respectively. In mutant ABM3, the sequence V⁶⁸⁹SNLTA was replaced with hexahistidine. The proteolytic processing sites identified at the C-terminus of purified Kgp variants by the nanoL-ESI-MS/MS analysis of tryptic digests are indicated by empty arrowheads. ABM1, ABM2, and ABM3 mutants were obtained by genomic integration of modified plasmid constructs using site-directed mutagenesis (QuickChange II XL Site Directed Mutagenesis Kit, Agilent Technologies, Santa Clara, CA, USA (Smith et al., 1990)). Briefly, master plasmid, pKgp/tetQ, used for site-directed mutagenesis was constructed based on the pUC19 vector. The TetQ cassette was amplified from plasmid pNFD13-2 using tetQSalIF (AAT AGT CGA CAC AAC GAA TTA TCT CCT TAA CGT) and tetQSpHIR (TTC GCA TGC TTT TAT TGC CAA GTT CTA ATG CT) primers and inserted into Sall and SphI sites in pUC19. A 5' fragment for homologous recombination included sequence corresponding to most of the *kgp* gene was amplified by PCR (Accuprime Pfx polymerase, Invitrogen) using *P. gingivalis* W83 genomic DNA as a template and primers KgpFrCXbaIF (GGT CTA GAG GTT CGT ATG CTT GTT GTT G) and KgpFrCSalIR (TAA TAG TCG ACC GAG TCC AAG ACA GAT T) and inserted to XbaI and SalI sites in the plasmid. Similarly, a 1.2-kb 3' flanking region of the *kgp* was amplified using primers KgpFrBSphI (TAG CAT GCG GAC TCG GAG ACT TTG TG) and KgpFrBHindR (ACC TAAG CTT CAA AGC ATC ACA GTA TAA G) and ligated into SphI and HindIII sites. The *kgp* gene sequence encoding the ABM in the master plasmid pKgp/tetQ was modified by QuickChange II XL site-directed mutagenesis method using three sets of oligonucleotide primers: ABM1_F: CAGGTAGGTGAGCCTCATCACCATCACCATCACAGCCCCTACCAGCCC and ABM1_R: GGGCTGGTAGGGGCTGTGATGGTGTGATGGTGTGATGAGGCTCACCTACCTG; ABM2_F: GTAGGTGAGCCTAGCCCCCAT CACCATCACCATCACTACCAGCCCGTTTCCAACCTG and ABM2_R: CAAGTTGGAAACGGGCTGGTAGTGTGATGGTGTGATGGTGA TGGGGGCTAGGCTCACCTAC; ABM3_F: AGCCCTACCAGCCCCATCACCATCACCATCACACAACGCAGGGTCAGAAAG and ABM3_R: CTTTCTGACCCTGCGTTGTGTGATGGTGTGATGGTGTGATGGGGCTGGTAGGGGCT, each containing the desired mutation and *PfuUltra* high-fidelity (HF) DNA polymerase, according to manufacturer's instructions. Obtained pKgp/ABM1, pKgp/ABM2 and pKgp/ABM3 plasmids were used for generation of isogenic mutants via homologous recombination in *P. gingivalis*. Genomic integration by a double crossover event was confirmed by PCR and verified by DNA sequencing of the entire *kgp* gene in the mutants.

was characterized in comparison to the wild-type parental strain.

The *kgp* gene mutation had no effect on Rgp activity and subcellular distribution. In the mutants, the vast majority of Rgps are cell-associated as in the wild-type strain. However, ABM mutants produced approximately only one-third total

Kgp activity of the parental strain and in stark contrast to the wild-type strain, this activity was found almost exclusively in a soluble form in the growth medium regardless of the age of the culture (Figure 2). This decreased production of Kgp was not related to hindered gene expression since qRT-PCR analysis revealed the same level the *kgp* gene transcription

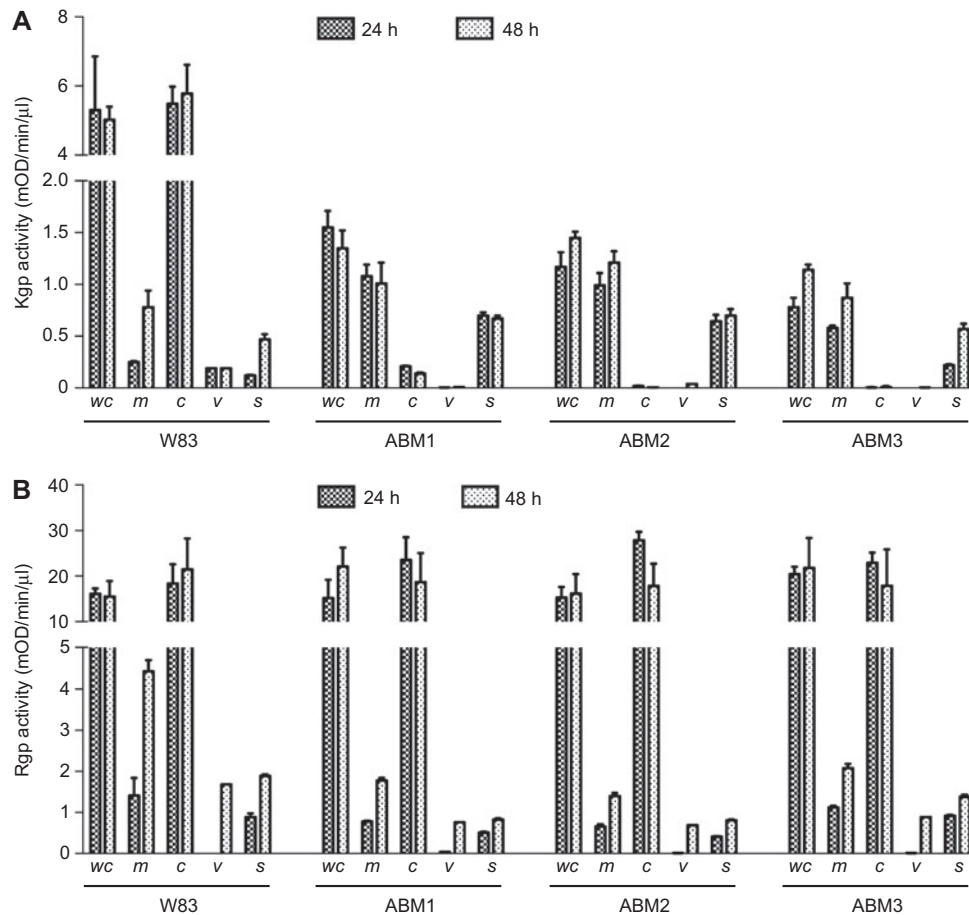


Figure 2 Kgp (A) and Rgp (B) activity in whole culture (wc), growth medium (m), collected washed cells (c), vesicles (v), and particle-free growth medium (s) of wild type *P. gingivalis* W83 and mutant strains ABM1, ABM2 and ABM3.

The strains were cultivated into late exponential/early stationary (24 h) and late stationary (48 h) phase of growth as described by Johnson and colleagues (Johnson et al., 2011). Cultures were adjusted to the same $OD_{600}=1.5$ and cells collected by centrifugation (5000 g, 20 min) washed and resuspended to the original volume to obtain the washed cells fraction (c). The growth media (m) was subjected to ultracentrifugation (100 000 g, 60 min). The obtained pellet was resuspended in TBS (v, vesicles) while the supernatant constituted particle-free growth medium (s). In each fraction, Kgp and Rgp activity was determined using Ac-Lys-pNA and Bz-Arg-pNA, respectively. Of note, mutations did not affect the growth rate of *P. gingivalis*.

in mutants and in the parental strain (data not shown). As disintegration of bacteria by sonication did not release any additional Kgp activity, we assumed that lower level of Kgp activity produced by the ABM mutants is due to disturbed folding and impaired maturation of Kgp due to added hexahistidine motif. To assess this possibility, we have subjected the mutants to Western blot analysis.

In accordance with the cellular distribution of Kgp activity in the ABM mutants, a single band representing the Kgp catalytic domain (Kgp_{cat}) was located exclusively in the media fraction but absent from cell extracts (Figure 3A) in Western blot using Kgp_{cat} -specific mAbs. Interestingly, cell extracts of *P. gingivalis* cultured only for 24 h revealed the presence of additional weak but clear bands of molecular mass higher than the Kgp_{cat} in the ABM mutants (Figure 3B). The highest band (200 kDa) in ABM2 cell extract may represent a full-length proKgp while the others are proKgp-derived fragments containing Kgp_{Pcat} . No such bands were found in the wild-type *P. gingivalis* regardless of the culture age. Therefore,

the presence of intermediate forms of Kgp in cell extracts of ABM mutants suggests that indeed, a portion of mutated *kpg* translation products were misfolded and were inefficiently processed explaining why mutants produce less Kgp activity than the wild-type *P. gingivalis* strain. In concordance with unaffected Rgp activity and cellular distribution, mutations in Kgp had no effect on Rgps band patterns (Figure 3C).

The partially processed Kgp was also detected in 24 h culture medium of ABM2 and ABM3 mutants (Figure 3B). Western blots with anti-hexahistidine antibodies revealed strong immunoreactive bands only in the media from ABM1 and ABM3 mutants and barely visible band in the ABM2 mutant (Figure 3D) arguing that proKgp polypeptide proteolytic processing occurs downstream of hexahistidine tag in the former two mutants and mostly within or upstream of the tag in the latter strain. Similarly, two higher molecular mass (60- and 70-kDa) forms of Kgp bearing the hexahistidine tags were detected in the media of ABM3 mutant cultured for 24 h (Figure 3E).

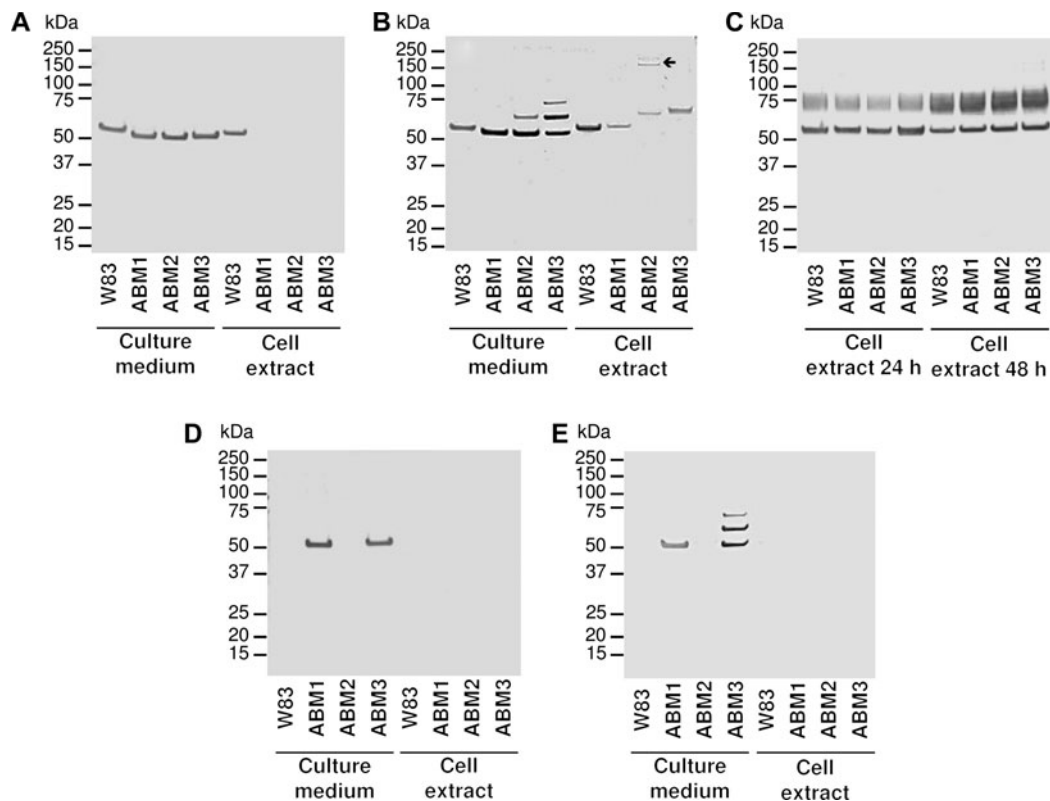


Figure 3 Western blot analysis of media and the whole cell fractions derived from wild-type *P. gingivalis* W83 and isogenic ABM mutants cultivated for 24 h (B, E) or 48 h (A, C, D) for the presence of Kgp (A and B), Rgps (C), and hexahistidine tag (D and E).

For fraction separation, see Figure 2 legend. Proteins in 20 μ l of original samples were resolved on 4–12% Bis-Tris SDS-PAGE gels and electrotransferred onto nitrocellulose membranes. After blocking non-specific binding sites, membranes were probed with mAb anti-Kgp (panels A and B), rabbit pAb anti-Rgp (panel C), rabbit pAb anti-6His tag (GenScript, Atlanta, GA, USA) (panels D and E), then secondary antibodies conjugated with alkaline phosphatase and specific bands were visualized with AP conjugate Substrate Kit (BioRad, Hercules, CA, USA). Arrowhead in panel B indicates full length proKgp.

The presence of His-tags on Kgp secreted by ABM1 and ABM3 mutants allows for their affinity purification on Ni-Sepharose (Figure 4A). Surprisingly, only a small fraction (6–7%) of the total Kgp activity was recovered from Ni-Sepharose after ABM1 and ABM3 media were applied onto Ni-chelating matrix. The bulk of Kgp was found unbound in the Ni-Sepharose flow-through fraction. Western blot analysis of bound and unbound Kgp forms separated on the affinity column clearly showed that the latter sample did not interact with anti-hexahistidine antibody (Figures 4B and 4C). The lack of interaction with anti-6His antibody and Ni-Sepharose was found to be due to the lack of hexahistidine motif as inferred from nanoL-ESI-MS/MS analysis of the unbound forms of Kgp. Tryptic-digests of Ni-Sepharose bound Kgp forms returned QIQVGEPHHHHHH and QIQVGEPSPYQPHHHHHH peptides in proteins produced by ABM1 and ABM3 mutants, respectively. In stark contrast, in the unbound Kgp variants from all three mutants, no peptides containing the hexahistidine motif were identified. Interestingly, peptides bearing mono- and/or dihistidine at the C-terminus [QIQVGEPH(H), QIQVGEPSSH(H) and QIQVGEPSPYQPH(H)] were found in unbound Kgp produced by ABM1, ABM2, and ABM3 mutants, respectively. In addition, peptides with tetrahistidine (QIQVGEPHHHH and

QIQVGEPSPYQPHHHH) were also identified in unbound Kgp from the ABM1 and ABM3 mutants. Results of the nanoL-ESI-MS/MS analysis are in agreement with reactivity of these forms with polyclonal Abs reactive with tetra-, penta- and hexahistidine (Figure 4B) but not with monoclonal Abs specific only for the hexahistidine tag (Figure 4C).

All forms of Kgp obtained by affinity-chromatography and purified by ion-exchange and gel-filtration chromatography from Ni-Sepharose non-binding fraction were subjected to Edman degradation. Regardless which mutant the 50 kDa band was derived from, the same N-terminal sequence of the mature Kgp catalytic domain was found (DVYTDHGDLYNT). Conversely, no sequence was detected in the 60- and 70-kDa forms isolated from the ABM3 mutant, suggestive of a blocked N-terminus. Therefore, 50-, 60-, and 70-kDa protein bands were analyzed by MS to verify protein identity. In tryptic digests of the 70 kDa band, peptides derived from the entire Kgp profragment and catalytic domain were identified. One hundred and ten N-terminal residues of the profragment were missing in the 60 kDa form. Finally, no peptides derived from the profragment were found in the 50 kDa form. Together, it is clear that Kgp isoforms purified from the ABM3 mutant media represent the Kgp catalytic domain alone (50 kDa), with intact (70 kDa) and

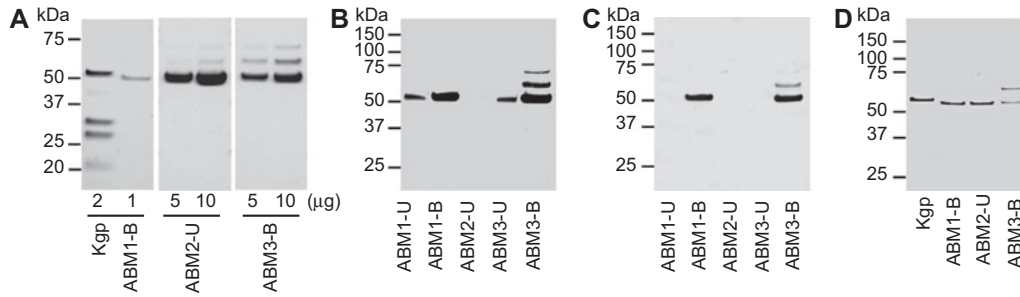


Figure 4 SDS-PAGE (A), Western blot analysis (B and C) and active site probing (D) of soluble forms of Kgp isolated from culture media of isogenic ABM mutants of *P. gingivalis* cultivated for 24 h.

Growth media were dialyzed against binding buffer (20 mM Na-Phosphate, 500 mM NaCl, 20 mM imidazole, 0.02% NaN_3 , pH 7.4) and incubated with Ni^{2+} -Sephacrose 6 Fast Flow (GE Healthcare, Pittsburgh, PA, USA) slurry with continuous rotation overnight at 4°C. Ni^{2+} -Sephacrose beads were collected by centrifugation (1000 g, 10 min), washed with the binding buffer and bound protein eluted with 500 mM imidazole. The supernatant was used to purify remaining bulk of Kgp activity. To this end, the supernatant was passed through DE-52 to remove hemin then the enzyme was further purified by gel filtration on Superdex 75 followed by ion-exchange chromatography on a Mono Q column (ACTA). In obtained fractions protein content was determined by the BCA method using bovine serum albumin as a standard. The high molecular weight Kgp complex isolated from strain HG66 (1 μg) and indicated amounts of protein (ABM-U, Kgp non-binding to Ni^{2+} -Sephacrose and purified by conventional chromatography; ABM-B, Kgp purified on Ni^{2+} -Sephacrose) were subjected to SDS-PAGE (Panel A), Western blot analysis (5 μg) (Panels B and C) and active-site probing (Panel D). For the latter analysis samples were pretreated with AcKbio-Y-hex-KAOMK (Kato et al., 2005) at 10 μM final concentration for 30 min at room temperature. The reaction was stopped by addition of TLCK to 10 mM concentration. All samples were treated with reduced sample buffer, denatured at 100°C and resolved on 4–12% Bis-Tris SDS-PAGE gels. For Western blot and activity probing resolved proteins were electrotransferred onto nitrocellulose membranes. After blocking, membranes were probed with rabbit pAb anti-6His tag (GenScript, Santa Clara, CA, USA reacts with tetra-, penta- and hexa-histidine) (Panel B), mAb anti-6His tag (Roche, Indianapolis, IN, USA detects exclusively hexahistidine) (Panel C) and streptavidin-alkaline phosphatase conjugate (Panel D). Blots were developed with AP conjugate Substrate Kit (BioRad, Hercules, CA, USA).

truncated profragment (60 kDa). As shown by nearly identical K_m and k_{cat} values (Table 1), the soluble fully processed Kgp_{cat} released by mutants have the same catalytic activity on Ac-Lys-pNA and Z-Lys-pNA synthetic substrates as the native 110 kDa Kgp purified from *P. gingivalis* HG66 growth medium, which is the full protein complex comprising of the catalytic and HA domains (Pike et al., 1994).

Presence of the profragment in the 70- and 60-kDa forms of Kgp prompted us to investigate if they are proteolytically active. To this end, affinity purified Kgp forms secreted by the ABM1, ABM2, and ABM3 mutants were treated with an active site probe, a biotinylated irreversible Kgp-specific inhibitor (Kato et al., 2005). In this reaction, only 50- and

60-kDa Kgp forms but not 70-kDa band (Figure 4) were labelled arguing that the full length profragment exerts latency on Kgp activity.

The molecular weight of hexahistidine labelled or unlabelled 50 kDa forms derived from different ABM mutants is indistinguishable by SDS-PAGE but visibly lower than that of Kgp_{cat} in wild-type *P. gingivalis* W83 (Figure 3) or derived from the enzyme purified from the HG66 strain (Figure 4). Along with similar K_m and k_{cat} values between the wild-type Kgp and the hexahistidine-inserted Kgp variants, it can be inferred that insertion of the tag into ABM interferes with a normal proteolytic processing but has no deleterious effect on folding of the Kgp catalytic domain. As indicated by the

Table 1 Kinetic constants for substrates turnover by the multidomain Kgp purified from strain HG66 and the catalytic domain alone produced by the ABM1 mutant.

Enzymes	Substrates					
	Ac-Lys-pNA			Z-Lys-pNA		
	k_{cat} (s^{-1})	K_m (μM)	k_{cat}/K_m ($\text{mM}^{-1}\text{s}^{-1}$)	k_{cat} (s^{-1})	K_m (μM)	k_{cat}/K_m ($\text{mM}^{-1}\text{s}^{-1}$)
Kgp HG66	1.65±0.08	140.1±8.3	11.8±1.3	1.04±0.1	188.5±26.1	5.7±1.3
Kgp ABM1	0.99±0.02	98.7±2.2	10.1±0.1	0.92±0.06	147.7±9.2	6.22±0.21

$n=3$; $\pm\text{SD}$.

The kinetic constants k_{cat} , K_m and k_{cat}/K_m were determined for the N- α -acetyl-L-Lysine-*p*-nitroanilide (Ac-Lys-pNA, Bachem) and N- α -carbobenzoxy-L-Lysine-*p*-nitroanilide (Z-Lys-pNA, Novabiochem). Kgp (20–40 nM) was incubated in assay buffer (200 mM Tris, 5 mM CaCl_2 , 150 mM NaCl, and 0.02% NaN_3 , pH 7.6) supplemented with 10 mM L-cysteine. After 10 min at 37°C, chromogenic substrates Ac-Lys-pNA or Z-Lys-pNA were added at various concentrations (0–500 μM) and the release of *p*-nitroanilide was monitored spectrophotometrically at 405 nm (Spectramax M5 spectrophotometer plate reader, Molecular Devices). k_{cat} and K_m were calculated by non-linear regression using Graphpad Prism software version 5 (GraphPad Software, La Jolla, USA). The specific activity of Kgp ABM1 and other Kgp forms produced by ABM1 and ABM2 mutants and purified on the analytical scale was practically the same. Therefore, we assumed that substrate hydrolysis by these Kgp variants occurs with the same kinetic constants as those determined for Kgp ABM1.

nanoL-ESI-MS/MS analysis of the purified Kgp forms, the aberrant promiscuous proteolysis apparently occurred at a number of sites directly after (Ni-Sepharose bound forms) and within the hexahistidine sequence (Ni-Sepharose unbound forms) (Figure 1D). Generated in this way, C-terminally truncated Kgp variants have molecular weight indistinguishable one from the other in SDS-PAGE but clearly lower than that of wild-type Kgp as proteolysis occurred at least several residues upstream from the native cleavage site in the wild-type protein (Figure 1). Subsequently, the major part of the oligomerization motif was lost and the Kgp catalytic domain was released into the medium together with the truncated or intact profragment. Apparently, the remaining N-terminal fragment of the oligomerization motif GEPSP and GEPSPYQP in ABM2 and ABM3, respectively, is insufficient to mediate oligomerization of the catalytic domain to the hemagglutinin/adhesin domains. Of note, the mode of association of the Kgp/RgpA complex on the *P. gingivalis* surface is unclear. Nevertheless, it can be hypothesized that glycosylated HA4 anchors the remaining domains to the outer membrane of the organism. The presence of the conservative C-terminal domain (CTD) essential for RgpB glycosylation and anchorage in the outer membrane (Nguyen et al., 2007) in RgpA and Kgp supports this hypothesis.

Cumulatively, we have confirmed the ABM role in oligomerization of the catalytic and HA domains of Kgp into the non-covalent complex. Alteration of the ABM leads to aberrant proteolysis at the junction between proKgp_{cat} and HA1, resulting in secretion of the soluble catalytic domain. The mutated Kgps are truncated at the C-terminus in comparison to wild-type Kgp but with catalytic properties indistinguishable from the native, multidomain Kgp_{cat}-HA complex. Purification of the Kgp catalytic domain alone opens the possibility to solve the crystal structure of this gingipain and investigate the role of HA domains in Kgp function as the major virulence factor of *P. gingivalis*.

Acknowledgements

This work was supported by grants from: the National Institutes of Health, USA (R01 Grants DE 09761 and EB005011) (to JP and MB, respectively), National Science Center (2011)/01/B/NZ6/00268, Kraków, Poland) (to JP), the European Community (FP7-HEALTH-2010-261460 "Gums&Joints") (to JP and JJE), and the Foundation for Polish Science (TEAM project DPS/424-329/10) (to J.P.). The Faculty of Biochemistry, Biophysics and Biotechnology of the Jagiellonian University is a beneficiary of structural funds from the European Union (POIG.02.01.00-12-064/08).

References

Albandar, J.M. and Rams, T.E. (2002). Global epidemiology of periodontal diseases: an overview. *Periodontol.* 2000 29, 7–10.
 Bhogal, P.S., Slakeski, N., and Reynolds, E.C. (1997). A cell-associated protein complex of *Porphyromonas gingivalis* W50 composed of Arg- and Lys-specific cysteine proteinases and adhesins. *Microbiology* 143, 2485–2495.

Cobb, C.M., Williams, K.B., and Gerkovitch, M.M. (2009). Is the prevalence of periodontitis in the USA in decline? *Periodontol.* 2000 50, 13–24.
 Guo, Y., Nguyen, K.A., and Potempa, J. (2010). Dichotomy of gingipains action as virulence factors: from cleaving substrates with the precision of a surgeon's knife to a meat chopper-like brutal degradation of proteins. *Periodontol.* 2000 54, 15–44.
 Johnson, N.A., McKenzie, R.M., and Fletcher, H.M. (2011). The *bcp* gene in the *bcp-recA-vimA-vimE-vimF* operon is important in oxidative stress resistance in *Porphyromonas gingivalis* W83. *Mol. Oral. Microbiol.* 26, 62–77.
 Kato, D., Boatright, K.M., Berger, A.B., Nazif, T., Blum, G., Ryan, C., Chehade, K.A., Salvesen, G.S., and Bogoy, M. (2005). Activity-based probes that target diverse cysteine protease families. *Nat. Chem. Biol.* 1, 33–38.
 Kozarov, E., Whitlock, J., Dong, H., Carrasco, E., and Progulsk-Fox, A. (1998). The number of direct repeats in *hagA* is variable among *Porphyromonas gingivalis* strains. *Infect. Immun.* 66, 4721–4725.
 Mikolajczyk-Pawlinska, J., Kordula, T., Pavloff, N., Pemberton, P.A., Chen, W.C., Travis, J., and Potempa, J. (1998). Genetic variation of *Porphyromonas gingivalis* genes encoding gingipains, cysteine proteinases with arginine or lysine specificity. *Biol. Chem.* 379, 205–211.
 Nguyen, K.-A., Travis, J., and Potempa, J. (2007). Does the importance of the C-terminal residues in the maturation of RgpB from *Porphyromonas gingivalis* reveal a novel mechanism for protein export in a subgroup of Gram-negative bacteria? *J. Bacteriol.* 189, 833–843.
 O'Brien-Simpson, N.M., Pathirana, R.D., Walker, G.D., and Reynolds, E.C. (2009). *Porphyromonas gingivalis* RgpA-Kgp proteinase-adhesin complexes penetrate gingival tissue and induce proinflammatory cytokines or apoptosis in a concentration-dependent manner. *Infect. Immun.* 77, 1246–1261.
 Pathirana, R.D., O'Brien-Simpson, N.M., Veith, P.D., Riley, P.F., and Reynolds, E.C. (2006). Characterization of proteinase-adhesin complexes of *Porphyromonas gingivalis*. *Microbiology* 152, 2381–2394.
 Pathirana, R.D., O'Brien-Simpson, N.M., Visvanathan, K., Hamilton, J.A., and Reynolds, E.C. (2008). The role of the RgpA-Kgp proteinase-adhesin complexes in the adherence of *Porphyromonas gingivalis* to fibroblasts. *Microbiology* 154, 2904–2911.
 Pavloff, N., Potempa, J., Pike, R.N., Prochazka, V., Kiefer, M.C., Travis, J., and Barr, P.J. (1995). Molecular cloning and structural characterization of the Arg-gingipain proteinase of *Porphyromonas gingivalis*. Biosynthesis as a proteinase-adhesin polyprotein. *J. Biol. Chem.* 270, 1007–1010.
 Pavloff, N., Pemberton, P.A., Potempa, J., Chen, W.C., Pike, R.N., Prochazka, V., Kiefer, M.C., Travis, J., and Barr, P.J. (1997). Molecular cloning and characterization of *Porphyromonas gingivalis* lysine-specific gingipain. A new member of an emerging family of pathogenic bacterial cysteine proteinases. *J. Biol. Chem.* 272, 1595–1600.
 Pike, R., McGraw, W., Potempa, J., and Travis, J. (1994). Lysine- and arginine-specific proteinases from *Porphyromonas gingivalis*. Isolation, characterization, and evidence for the existence of complexes with hemagglutinins. *J. Biol. Chem.* 269, 406–411.
 Potempa, J., Pike, R., and Travis, J. (1995). The multiple forms of trypsin-like activity present in various strains of *Porphyromonas gingivalis* are due to the presence of either Arg-gingipain or Lys-gingipain. *Infect. Immun.* 63, 1176–1182.
 Slakeski, N., Bhogal, P.S., O'Brien-Simpson, N.M., and Reynolds, E.C. (1998). Characterization of a second cell-associated

- Arg-specific cysteine proteinase of *Porphyromonas gingivalis* and identification of an adhesin-binding motif involved in association of the prtR and prtK proteinases and adhesins into large complexes. *Microbiology* 144, 1583–1592.
- Smith, C.J., Parker, A., and Rogers, M.B. (1990). Plasmid transformation of *Bacteroides* spp. by electroporation. *Plasmid* 24, 100–109.
- Tam, V., O'Brien-Simpson, N.M., Pathirana, R.D., Frazer, L.T., and Reynolds, E.C. (2008). Characterization of T cell responses to the RgpA-Kgp proteinase-adhesin complexes of *Porphyromonas gingivalis* in BALB/c mice. *J. Immunol.* 181, 4150–4158.
- Tam, V., O'Brien-Simpson, N.M., Chen, Y.Y., Sanderson, C.J., Kinnear, B., and Reynolds, E.C. (2009). The RgpA-Kgp proteinase-adhesin complexes of *Porphyromonas gingivalis* inactivate the Th2 cytokines interleukin-4 and interleukin-5. *Infect. Immun.* 77, 1451–1458.
- Veith, P.D., Talbo, G.H., Slakeski, N., Dashper, S.G., Moore, C., Paolini, R.A., and Reynolds, E.C. (2002). Major outer membrane proteins and proteolytic processing of RgpA and Kgp of *Porphyromonas gingivalis* W50. *Biochem. J.* 363, 105–115.
- Veith, P.D., Chen, Y.Y., and Reynolds, E.C. (2004). *Porphyromonas gingivalis* RgpA and Kgp proteinases and adhesins are C terminally processed by the carboxypeptidase CPG70. *Infect. Immun.* 72, 3655–3657.

Received April 10, 2012; accepted May 6, 2012